

Algorithm for simulation of quantum many-body dynamics using dynamical coarse graining

M. Khasin and R. Kosloff

*Fritz Haber Research Center for Molecular Dynamics,
Hebrew University of Jerusalem, Jerusalem 91904, Israel*

(Dated: May 16, 2019)

Abstract

An algorithm for simulating the dynamics of a restricted set of observables of a many-body system is presented. The set comprises the spectrum-generating algebra (SGA) of observables of the system. The technical development of the algorithm is based on the close connection between the algebra of observables and the set of states minimizing the generalized uncertainty with respect to these observables – the generalized coherent states (GCS). These states serve as dynamical basis functions for expanding the state of the system. The original unitary dynamics of the observables is simulated by a surrogate open-system dynamics, which can be interpreted as a weak measurement of the elements of the SGA, performed on the evolving system. The measurement leads to a coarse-graining of the evolving state in the corresponding phase-space. The coarse-grained state can be represented as a mixture of pure states, localized in the phase-space. The evolution of the pure states is governed by the stochastic nonlinear Schrödinger equation (sNLSE), which can be simulated at dramatically lower computational cost using expansion of the localized solutions in the basis of the GCS. The algorithm is applied to the simulation of the dynamics of a system of $2 * 10^4$ cold atoms in the double-well trap, described by the two-sites Bose-Hubbard model.

PACS numbers: 03.67.Mn, 03.67.-a, 03.65.Ud, 03.65 Yz

I. INTRODUCTION

Simulation of quantum many-body dynamics is a challenging task [1]. The computational resources of solving the Schrödinger equation scale with the size of the Hilbert space. The effective Hilbert space dimension of a typical many-body system is huge. As a consequence, approaches based on a numerical solution of the corresponding Schrödinger equation are practically excluded. Typical approximate solutions rely on limiting the extent of quantum many-body correlations, as for example in various mean-field approximations. An alternative is to restrict the scope of the simulation to a subset of observables. In the present study we describe a method of simulation which is restricted to a subset of dynamical observables. This restriction allows to develop an efficient and converged algorithm for the dynamics of this subset of observables.

To demonstrate the approach we apply the algorithm to the simulation of the dynamics of $N = 2 * 10^4$ cold atoms in a double-well trap [2, 3, 4, 5]. The system is modeled by the two-site Bose-Hubbard model [6] with the Hamiltonian:

$$\hat{H} = -\Delta \sum_{i=1,2} (\hat{a}_{i+1}^\dagger \hat{a}_i + \hat{a}_i^\dagger \hat{a}_{i+1}) + \frac{U}{2N} \sum_{i=1,2} (\hat{a}_i^\dagger \hat{a}_i)^2, \quad (1)$$

where \hat{a}_i (\hat{a}_i^\dagger) is the creation (annihilation) operator of a particle in the i -th well. Δ describes the hopping rate and U scales the two-body interaction. The transformation to the operators

$$\begin{aligned} \hat{J}_x &= \frac{1}{2}(\hat{a}_1^\dagger \hat{a}_2 + \hat{a}_2^\dagger \hat{a}_1) \\ \hat{J}_y &= \frac{1}{2i}(\hat{a}_1^\dagger \hat{a}_2 - \hat{a}_2^\dagger \hat{a}_1) \\ \hat{J}_z &= \frac{1}{2}(\hat{a}_1^\dagger \hat{a}_1 - \hat{a}_2^\dagger \hat{a}_2) \end{aligned} \quad (2)$$

leads to the following Lie-algebraic form of the Hamiltonian

$$\hat{H} = -\omega \hat{J}_x + \frac{U}{N} \hat{J}_z^2, \quad (3)$$

where $\omega = 2\Delta$. The set of single-particle operators $\{\hat{J}_x, \hat{J}_y, \hat{J}_z\}$ is closed under the commutation relation and spans the $\mathfrak{su}(2)$ spectrum-generating algebra [7] of the system. The observables: $\hat{J}_x, \hat{J}_y, \hat{J}_z$ are the target of the dynamical simulation, representing coherence, current and population difference between the wells.

The Hilbert space of the system of N atoms carries the $N + 1$ dimensional irreducible representation [8] of the the spectrum-generating $\mathfrak{su}(2)$ algebra, corresponding to the pseudo-spin quantum number $j = N/2$. A numerical solution of the corresponding Schrödinger

equation requires multiplication of the $N + 1$ -dimensional state vector of the system by the $(2N + 1) \times (2N + 1)$ matrix of the Hamiltonian. In order to propagate to a time scale of ω^{-1} $O(N)$ such multiplications are needed. As a result, the propagation of the state vector requires $O(N^3)$ elementary operations from which any expectation value can be calculated [9]. The memory resources for the storage of the $(2N + 1) \times (2N + 1)$ matrices with the double precision is $O(10N^2)$ bytes. Taking $N = 2 * 10^4$ brings the memory requirements to the edge of the $2Gb$ RAM capacity of a regular modern computer. Having $N = 10^5$ will make it prohibitive to store the Hamiltonian matrix in the RAM. The challenge of an efficient simulation is that the computational resources become independent of the Hilbert space dimension.

The basic idea of the algorithm [13] stems from the close connection between an algebra of observables and the generalized coherent states [8] which minimize the generalized uncertainty with respect to these observables. These states serve as dynamical basis functions for expanding the state of the system. The second ingredient of the algorithm [13] is to replace the original unitary dynamics generated by Eq. (3) by a certain surrogate dynamics. This surrogate dynamics is an open-system dynamics, corresponding to a weak measurement performed on the original system. The simulation of the open-system evolution is realized by averaging the pure-state dynamics generated by the *stochastic nonlinear Schrödinger equation*(sNLSE)[10, 11, 12] over the stochastic realizations. The sNLSE corresponds to a single realization of the process of weak measurement of the elements of the spectrum generating algebra (2) performed on the system, evolving under the Hamiltonian (3). If the measurement is sufficiently strong, the computational complexity of the sNLSE is dramatically smaller than complexity of solving the corresponding Schrödinger equation. As a consequence, the numerical solution of the sNLSE becomes practical.

The expectation values of observables are obtained by averaging over the stochastic realizations. The number of realizations for a prescribed relative error is independent of N , therefore asymptotically the complexity of the simulation is determined by the cost of solving the sNLSE. The parameter of the sNLSE, corresponding to the strength of the measurement, is decreased until the open dynamics of the single-particle observables (2) converges to the original *unitary* dynamics, driven by the Hamiltonian (3). It is shown that the convergent solution is obtained at the values of the measurement strength which is still sufficient for a drastic reduction of the computational complexity of the sNLSE, compared to the

Schrödinger equation.

The reduction of the computational complexity is achieved by virtue of the localization of the solution of the sNLSE of the system in the corresponding phase space under the action of the measurement [13, 14]. On the level of the density matrix the localization leads to a coarse-graining of the phase-space representation of the state, destructing the fine structure but leaving unaffected the dynamics of smooth observables, such as the single-particle observables.

The localization of the sNLSE solution leads to compression of the size of the time-dependent computational basis of the simulation. The multiplication of $N \times 1$ state vector by a $N \times N$ matrix necessary for the propagation of the Schrödinger equation, is replaced by multiplication of $M \times 1$ state vector by a $M \times M$ matrix, where the number $M \ll N$ is asymptotically independent on N . In the application, considered in Section III B, $M \approx 3 * 10^{-3}N$. This spectacular compression of the computational basis results in dramatic speed-up of the computation by the order of 10^3 and reduction of the involved RAM resources by the factor of 10^5 .

Section II outlines the basic ideas in the foundation of the algorithm. It summarizes the main results of Refs.[13, 14] and applies them to construction of an algorithm for simulation of quantum dynamics, driven by the $\mathfrak{su}(2)$ -Hamiltonians.

Section III focuses on the application of the algorithm to the Bose-Hubbard model. Discussion and conclusions are presented in Section IV.

II. THE ALGORITHM

A. Generalal considerations

The algorithm for simulation of a many-body quantum dynamics, is based on the following sequence of steps [13]:

1. The choice of the time-dependent computational basis, built of the generalized coherent states (GCS), associated with the spectrum-generating algebra (SGA) of the system.
2. The choice of the elements of the SGA of the system as the distinguished set of observables for the simulation.

3. Numerical solution of the stochastic Nonlinear Schrödinger Equation (sNLSE), corresponding to the weak measurement of the elements of the SGA, performed on the evolving system.
4. Averaging of the expectation values of the SGA observables over many different stochastic realizations.
5. Decreasing the strength of measurement to obtain convergence of the open-system dynamics of the SGA observables to the original unitary evolution.

1. *The choice of the time-dependent basis*

The motivation for the algorithm is the following definition of the efficient simulation of a quantum many-body dynamics:

Definition: *The simulation of dynamics of a Lie algebra of observables of the system is efficient if and only if the necessary memory and the CPU resources for the computation do not depend on the Hilbert space (irreducible) representation of the algebra.*

An example of the efficient simulation is the solution of the Heisenberg equations of motion for the algebra elements, when the Hamiltonian is itself an element of the algebra. Another example is a mean field solution of the quantum dynamics, i.e., solution of the variational equations of motion for the ansatz, parametrized by the expectation values of the operators, belonging to the algebra [15].

The starting point for the algorithm is the assumption that reduction of the computational complexity is achieved by using a time-dependent basis of a small number of states. It is further assumed that the many-body Hamiltonian is given in terms of the spectrum-generating algebra $SGA = span \{ \hat{X}_i \}$ of the system as in Eq.(3).

A necessary ingredient of a simulation scheme is a calculation of the matrix elements of the Hamiltonian in the time-dependent basis. Let $\psi_i(t)$ be the time-dependent computational basis. Let the Hilbert space dimension be n . Then the state vector of the system becomes

$$|\Psi(t)\rangle = \sum_{i=1}^M c_i(t) |\psi_i(t)\rangle = \sum_{i=1}^M c_i(t) \hat{U}_i(t) |\psi_i(0)\rangle, \quad (4)$$

where $M \leq n$ and $\hat{U}_i(t)$ is a non unique time-dependent unitary transformation of the reference state $\psi_i(0)$. An efficient computation of the matrix elements of the Hamiltonian

in the time-dependent basis $\langle \psi(t)_i | \hat{H} | \psi(t)_j \rangle$ implies that the following transformation is performed efficiently:

$$\hat{H} \rightarrow \hat{U}_i(t) \hat{H} \hat{U}_j(t) \quad (5)$$

and, in particular, the unitary transformation

$$\hat{H} \rightarrow \hat{U}_i(t) \hat{H} \hat{U}_i(t). \quad (6)$$

is performed efficiently. By the assumption, the Hamiltonian is given as a function of the SGA operators \hat{X}_i . Efficient transformation (6) implies that the transformation of \hat{X}_i under the action of $\hat{U}_j(t)$ is performed efficiently. It follows that $\hat{U}_j(t)$ is generated by the SGA itself.

In that case, each $\psi_i(t)$ in Eq.(4) can be represented as an orbit of the reference state $\psi_i(0)$ under the action of the SGA:

$$\psi_i(t) = e^{i \sum_i x_i(t) \hat{X}_i} \psi_i(0), \quad (7)$$

$$\hat{X}_i \in SGA. \quad (8)$$

According to the definition [8, 16] the $\psi_i(t)$ is a *generalized coherent state* (GCS), associated with the SGA and the reference state $\psi_i(0)$. Therefore, the time-dependent computational basis is a basis of the GCS, associated with the SGA of the system.

The choice of the reference states $\psi_i(0)$ affects the computational complexity of the simulation. The matrix elements $\langle \psi_i(0) | \hat{H} | \psi_j(0) \rangle$ and, therefore, the matrix elements $\langle \psi_i(0) | \hat{X}_k | \psi_j(0) \rangle$ must be computed efficiently. Generally, complexity of the computation of $\langle \psi_i(0) | \hat{X}_k | \psi_j(0) \rangle$ will depend on the Hilbert space representation of the SGA. Nonetheless, if the reference state $\psi_i(0)$ is chosen as the maximal (minimal) weight state of the representation, the computation can be performed group-theoretically [8], i.e., efficiently. These considerations lead to the choice of the basis of the GCS, associated with the SGA of the system and the maximal (minimal) weight state of the representation, as the time-dependent computational basis.

2. *The choice of the SGA observables for the simulation*

Given the ansatz (4) computation of the expectation value of an observables \hat{X} demands computing of $\langle \hat{X} \rangle = \langle \psi(t)_i | \hat{X} | \psi(t)_j \rangle$, i.e., performing the transformation

$$\hat{X} \rightarrow \hat{U}_i(t) \hat{X} \hat{U}_j(t). \tag{9}$$

In the previous subsection we found that $\hat{U}_i(t)$ is generated by the SGA. For efficient computation of $\langle \hat{X} \rangle$ it is necessary that the transformation (9) is independent on the Hilbert space representation of the SGA. It follows that \hat{X} must be of the form:

$$\hat{X} = \sum_{i=1}^K a_i \hat{X}_i + \sum_{ij} b_{ij} \hat{X}_i \hat{X}_j + \dots \sum_{i_1, i_2, \dots, i_L} c_{i_1, i_2, \dots, i_L} \prod_{j=1}^L \hat{X}_{i_j}, \tag{10}$$

where each $1 \leq i_j \leq K = \dim\{SGA\}$ and L is a fixed number, independent on the representation of the SGA. In particular, the Hamiltonian of the system must have this form in order that an efficient simulation be possible. The elements \hat{X}_i of the SGA is the simplest choice of observables of the form (10).

3. *Solving the stochastic Nonlinear Schrödinger Equation*

For efficient simulation it is necessary that M in Eq.(4) be independent of the Hilbert space representation of the SGA. This implies in particular that $M \ll n$ as $n \rightarrow \infty$. Generic Hamiltonian, nonlinear in the SGA elements, is expected to take an initial state of a many-body system to a state Eq.(4), corresponding to $M = O(n)$. Therefore, a generic unitary dynamics cannot be simulated efficiently.

A possible solution has been proposed in Ref.[13]: a surrogate open-system dynamics can be found, simulating the unitary dynamics modulo the expectation values of the restricted set of observables – the elements of the SGA. The open-system dynamics corresponds to the process of weak measurement of the elements of the SGA, performed on the system of interest, evolving under the action of the original Hamiltonian.

The open-system evolution can be simulated using stochastic unraveling of the evolving density operator into pure-state evolutions (quantum trajectories), governed by the stochastic Nonlinear Schrödinger equation (sNLSE)[10, 11, 12]. The pure state, evolving along a quantum trajectory, can be expressed in the form Eq.(4), corresponding to $M \ll n$, provided the measurement is sufficiently strong.

4. Averaging

The expectation values of the SGA observables are calculated along the quantum trajectory for each stochastic realization of the sNLSE. Averaging over the stochastic realizations recovers the open-system dynamics of the observables. The number of realizations needed for convergence of the averaged values to a given relative error is independent of the Hilbert space representation of the SGA. Therefore, the averaging can be performed efficiently.

5. Convergence to the unitary evolution

As the strength of the measurement decreases the open-system dynamics of the SGA observables converges to the original unitary dynamics. If a certain generic condition on the SGA and its Hilbert space representation is satisfied [13], the open system follows the evolution on widely separated time-scales. Due to this time-scales separation the open-system dynamics of the SGA observables converges to the unitary evolution at the value of the measurement strength which is sufficient to ensure that $M \ll n$ in the expansion (4) of the pure-state solution of the corresponding sNLSE. Therefore, the unitary evolution of the SGA observables can be simulated at substantially lower computational cost. The question when and whether this reduction of the computational complexity amounts to an efficient simulation is left for Section IV.

B. A linear implementation

The algorithm outlined in the previous subsection can be implemented in a variety of ways. This is in part due to the non uniqueness of the transformations $\hat{U}_i(t)$ in Eq.(4) of the computational basis elements. In the present implementation we adopt the choice $\hat{U}_i(t) = \hat{U}_j(t) = \hat{U}(t)$, leading to the term *linear implementation*. In the linear implementation the pure-state solution of the sNLSE is represented by

$$|\Psi(t)\rangle = \sum_{i=1}^M c_i(t) \hat{U}(t) |\psi_i(0)\rangle, \quad (11)$$

where $\psi_i(0)$ is a fixed set of the GCS, associated with the SGA and a maximal(minimal) weight state of the Hilbert space representation of the algebra.

The advantage of this choice is that the numerical effort is reduced to solving a system of linear equations. This explains the term. The disadvantage is that the number of the elementary computer operations will necessarily depend on the Hilbert space dimension for reasons discussed in Section IV. Therefore, the linear implementation cannot in principle lead to an efficient simulation in the sense of our definition. Still, as will be demonstrated in Section III, the reduction of the computational complexity can be so dramatic, that the simulation of the many-body dynamics becomes feasible in the case where solving the Schrödinger equation is practically impossible.

An infinitesimal time step of the simulation is represented as a superposition of the linear transformation \hat{T}_1 of the state represented in the fixed instantaneous basis, i.e., the transformation of the vector c_i in Eq.(11) and a subsequent unitary transformation \hat{T}_2 of the basis itself. The transformation \hat{T}_1 corresponds to the physical (measurable) evolution of the state, driven by the sNLSE. The transformation \hat{T}_2 ensures that the evolving state remains localized in the Hilbert subspace spanned by the instantaneous basis. Connection of the infinitesimal unitary transformation \hat{T}_2 to $\hat{U}(t)$ in Eq.(11) is established by the following relation:

$$T_2 = \hat{1} - \hat{U}(t)' dt. \quad (12)$$

The time-dependent basis is chosen from the GCS, associated with the SGA as argued above. It is interesting that this updating of the basis can be viewed as an analog of the Schmidt decomposition [17] in the generalized entanglement setting [18].

C. Application to the $\mathfrak{su}(2)$ spectrum-generating algebra

The algorithm presented above can be given an intuitive geometric meaning in the special case of the SGA spanned by the operators \hat{J}_x , \hat{J}_y and \hat{J}_z satisfying the commutation relations

$$\left[\hat{J}_i, \hat{J}_j \right] = i\epsilon_{ijk} \hat{J}_k, \quad (13)$$

of the $\mathfrak{su}(2)$ algebra. Examples of a many-body quantum system with the $\mathfrak{su}(2)$ SGA include the Lipkin-Meshkov-Glick model of interacting fermions [19] and cold bosonic atoms in the double-well trap [20, 21] among others [7].

The GCS of the $\mathfrak{su}(2)$ (termed spin-coherent states) are represented by points in the phase space, associated with the algebra [22]. The phase-space globally is a two-dimensional sphere

and the GCS are parametrized by spherical coordinates, for example, by the azimuthal and the polar angles. The $2j+1$ dimensional Hilbert space, carrying an irreducible representation of the algebra, is spanned by a linearly independent basis of GCS, represented by $2j+1$ points on the sphere. A localized state can be expanded in a small fraction of the total basis, represented by points inside a relatively small portion of the phase-space.

The corresponding sNLSE reads:

$$d|\psi\rangle = -i\hat{H} dt |\psi\rangle - \gamma \sum_{i=1}^3 \left(\hat{J}_i - \langle \hat{J}_i \rangle_\psi \right)^2 dt |\psi\rangle + \sum_{i=1}^3 \left(\hat{J}_i - \langle \hat{J}_i \rangle_\psi \right) d\xi_i |\psi\rangle, \quad (14)$$

where \hat{H} is the Hamiltonian of the system and where the Wiener fluctuation terms $d\xi_i$ satisfy

$$\langle d\xi_i \rangle = 0, \quad d\xi_i d\xi_j = 2\gamma \delta_{ij} dt. \quad (15)$$

The parameter γ is the strength of the measurement of elements \hat{J}_x , \hat{J}_y and \hat{J}_z of the spectrum-generating $\mathfrak{su}(2)$ algebra of the system.

A Hamiltonian nonlinear in \hat{J}_x , \hat{J}_y and \hat{J}_z , represented by the first term in Eq.(14), leads to the delocalization of a generic initial localized state. The non unitary stochastic contribution of the evolution due to the measurement, represented by the last two terms in Eq.(14), leads to a localization [14]. Therefore, a single stochastic realization of the open system evolution can be viewed as a small spot on the sphere, involving each instant a small fraction of the GCS, moving stochastically in the phase space.

The infinitesimal linear transformation \hat{T}_1 includes two parts: the original Hamiltonian part and the non unitary part, which contains a stochastic and a deterministic element. Both elements depend on the instantaneous state of the system. Therefore, while the infinitesimal transformation \hat{T}_1 is a linear transformation, the superposition of these transformations is described by the nonlinear Eq.(14). The infinitesimal linear transformation \hat{T}_1 is performed on the instantaneous state of the system represented by a superposition of the states of the instantaneous fixed basis of the GCS.

The GCS basis must be updated at each time step. Practically, a different but physically equivalent transformation has been found to be more convenient. Instead of updating the basis to match the evolving state we update the state to match the fixed basis. Therefore, the unitary transformation \hat{T}_2 is performed on the state itself and the inverse transformation \hat{T}_2^{-1}

– on the Hamiltonian and other observables. The unitary transformation \hat{T}_2 is generated by the $\mathfrak{su}(2)$ elements \hat{J}_x , \hat{J}_y and \hat{J}_z and rotates the state to the position localized in the fixed basis of the GCS.

Let the initial state be a spin-coherent state, represented by the point at the south pole of the phase space. The expectation values of the operators \hat{J}_x and \hat{J}_z vanish in this state. An infinitesimal transformation \hat{T}_1 takes the state into a new position having finite expectation values of \hat{J}_x and \hat{J}_z . The purpose of the unitary transformation \hat{T}_2 is to rotate the state back to the position with vanishing expectation values of \hat{J}_x and \hat{J}_z . This rotation is performed by the $SU(2)$ group transformation and is equivalent to rotating of the density operator in the Hilbert-Schmidt space to ensure that the projection of the density operator on the algebra is spanned by the \hat{J}_z operator. This procedure is analogous to the Schmidt-decomposition of the state in the generalized entanglement setting [18] as pointed out above.

The back-rotation of the operators by the inverse transformation \hat{T}_2^{-1} can be performed analytically, knowing how the $\mathfrak{su}(2)$ algebra elements transform under the $SU(2)$ group itself.

The superposition of the two transformations $\hat{T}_2 \circ \hat{T}_1$ of the state results in a new state, still localized about the south pole. The convergence of the computation to the exact *open-system-dynamics* solution is obtained by increasing the size of the GCS basis until the evolution of the single-particle observables has ceased to change. The convergence of computation to the exact *unitary* evolution of the single-particle observables is obtained by decreasing the strength of the measurement until the evolution of the single-particle observables has ceased to be affected.

III. APPLICATION TO THE TWO-SITE BOSE-HUBBARD MODEL

A. Introduction

The gas of cold atoms (bosons) in a double-well trap [3, 4] is described by the two-site Bose-Hubbard model. The Hamiltonian (1) contains two terms: the one-body (linear) term responsible for the hopping of the atoms from one well to another and the two-body (nonlinear) or interaction term responsible for the on-site attraction or repulsion of the atoms. In the present application we consider repulsive interaction, measured by the coupling strength $2U/N$, where N is the total number of particles in the trap. The hopping rate is

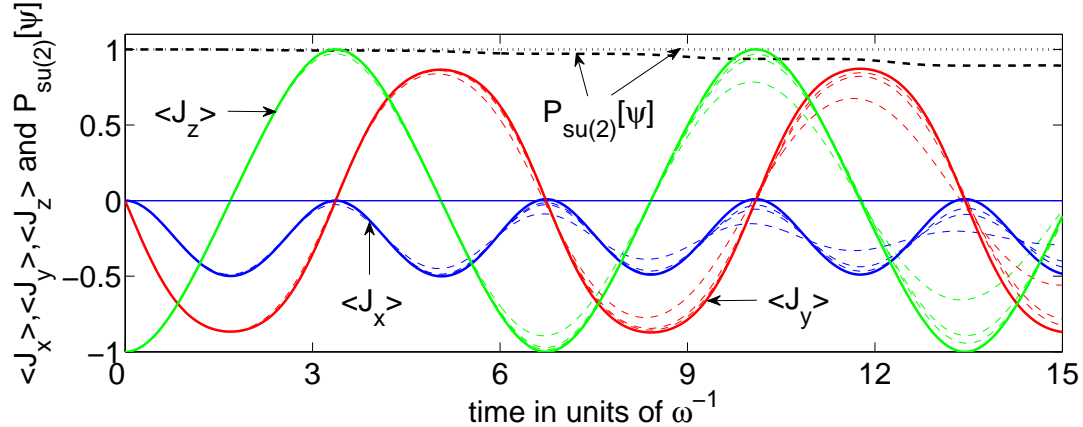


FIG. 1: (Color online) The mean-field solution for the expectation values of the single-particle observables \hat{J}_x (blue, solid), \hat{J}_y (red, solid) and \hat{J}_z (green, solid), Eq.(2), and the generalized purity (dotted), Eq.(16), as a function of time vs. the exact solution of the Schrödinger equation (dashed lines) for $N = 128, 256, 512$ (expectation values) and $N = 512$ (generalized purity). The system of N atoms resides initially in a spin-coherent state corresponding to the condensate prepared in the left well of the trap. The value of the on-site interaction is chosen $U/\omega = 1$. Time is measured in units of $\omega^{-1} = 0.5\Delta^{-1}$. The expectation values are normalized by the factor $j = N/2$. As the number of particles grows the exact solution approaches the mean-field solution on the characteristic time-scale of the oscillations.

fixed by the coefficient Δ of the one-body part.

The spectrum-generating algebra of the system is the $\mathfrak{su}(2)$ algebra of the single-particle operators (2). The system of N particles correspond to the $N + 1$ -dimensional irreducible representation of the algebra with the principle pseudo-spin quantum number $j = N/2$. Condensed state of the system is a generalized coherent state [21, 23], associated with the algebra, termed spin-coherent states in the literature [8, 22, 24].

The character of dynamics at fixed N depends on a single parameter U/ω , where $\omega = 2\Delta$. At $N \gg 1$ the weak interaction regime $U/\omega \leq 1$, corresponds to dynamics preserving coherence of the atomic condensate for times much larger than the the oscillation period of the population between the two wells [20]. High coherence corresponds to a weak delocalization, i.e., an initial spin-coherent state remains localized for a very long time. The corresponding dynamics is well described by solution of the mean-field variational equations of motion, assuming a spin-coherent state as the variational ansatz [15] (Fig.1).

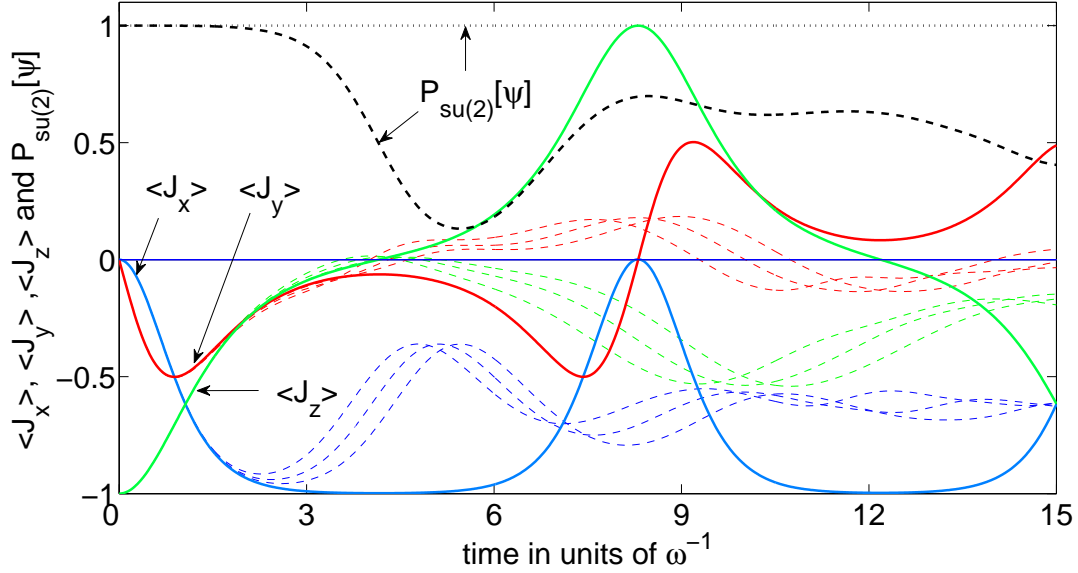


FIG. 2: (Color online) The mean-field solution for the expectation values of the single-particle observables \hat{J}_x (blue, solid), \hat{J}_y (red, solid) and \hat{J}_z (green, solid), Eq.(2), and the generalized purity (dotted), Eq.(16), for $N = 512$ as a function of time vs. the exact solution of the Schrödinger equation (dashed lines) for $N = 128, 256, 512$ (expectation values) and $N = 512$ (generalized purity). The system of N atoms resides initially in a spin-coherent state corresponding to the condensate prepared in the left well of the trap. The value of the on-site interaction is chosen $U/\omega = 2$, corresponding to the strong interaction regime. Time is measured in units of $\omega^{-1} = 0.5\Delta^{-1}$. The expectation values are normalized by the factor $j = N/2$. The mean-field approximation breaks down on the time-scale of a single oscillation.

When $U/\omega > 1$ the phase-space picture of the mean-field dynamics changes: an unstable fixed point appears and the associated separatrix [20]. The mean-field solution breaks down in the vicinity of the separatrix. As a consequence, an initial spin-coherent state prepared in the vicinity of the separatrix is expected to evolve into a delocalized state. The corresponding dynamics is characterized by the exponential loss of coherence [25] as measured by the purity of the single-particle density operator. This parametric regime is the hardest for the simulation and will be chosen to test the algorithm.

We choose the state of the condensate placed in one the wells for the (spin-coherent) initial state. This choice corresponds to the dynamics in the vicinity of the separatrix in the mean-field picture for $U/\omega = 2$ and large N [26]. Therefore, the choice $U/\omega = 2$ for the

interaction parameter has been made.

The loss of coherence can be measured by the generalized purity [18] of the state with respect to the $\mathfrak{su}(2)$ algebra of the single-particle observables. The generalized purity of the state ψ is defined by

$$P_{\mathfrak{su}(2)}[\psi] \equiv \sum_{i=x,y,z} \langle \hat{J}_i \rangle^2. \quad (16)$$

The generalized purity (16) equals unity if ψ is a spin-coherent state and is less than unity otherwise. A mean-field solution is a spin-coherent state by the definition. The mean-field approximation breaks down as the generalized purity decreases substantially.

Figs.1 and 2 show dynamics of the system of $N = 128, 256, 512$ particles corresponding to $U/\omega = 1$ and $U/\omega = 2$ respectively, obtained by a direct solution of the Schrödinger equation using the Chebyshev method [27]. Initial state of the system is chosen to be the condensed state of the atoms located in the left well. It is a spin-coherent eigenstate of the \hat{J}_z single-particle operator, measuring the difference of the right- and left-well populations of the atoms. The mean-field solution works well for the weak interaction regime $U/\omega = 1$, where the generalized purity of the evolving remains close to unity. In the case of $U/\omega = 2$, the purity decreases on the time-scale of a single oscillation of the condensate and the mean-field solution fails to reproduce correctly the character of the dynamics.

B. Application to a system of $N = 2 * 10^4$ cold atoms

1. Equations of motion

The numerical solution of the sNLSE (14) proceeds as a sequence of infinitesimal linear transformations:

$$|\psi\rangle \rightarrow \hat{T}_1 |\psi\rangle \quad (17)$$

$$|\psi\rangle \rightarrow \hat{T}_2 |\psi\rangle, \quad (18)$$

$$\hat{X} \rightarrow \hat{T}_2 \hat{X} \hat{T}_2^\dagger, \quad (19)$$

where \hat{X} stand for all relevant operators, i.e., the Hamiltonian and the single-particle observables, the linear transformation \hat{T}_1 drives the physical evolution of the state in the fixed computational basis of spin-coherent states and the unitary transformation \hat{T}_2 keeps the

state localized in the basis. The state ψ in Eqs.(17) and (18) is given by

$$|\Psi(t)\rangle = \sum_{i=1}^M c_i(t) |\psi_i(0)\rangle, \quad (20)$$

where $\psi_i(0)$ is the *fixed* computational basis of spin-coherent states. From Eq.(14)

$$\hat{T}_1 = \hat{I} + \left\{ -i\hat{H}dt - \gamma \sum_{i=1}^3 \left(\hat{J}_i - \langle \hat{J}_i \rangle_\psi \right)^2 dt + \sum_{i=1}^3 \left(\hat{J}_i - \langle \hat{J}_i \rangle_\psi \right) d\xi_i \right\}, \quad (21)$$

where $\langle \hat{J}_i \rangle$ are the instantaneous expectation values of the single-particle operators. From Eqs.(17), (21) and (4) we obtain

$$\begin{aligned} & \sum_{k=1}^M C_{jk} dc_k \\ &= \sum_{k=1}^M \left\{ -i(\hat{H})_{jk}dt - \gamma \sum_{i=1}^3 \left((\hat{J}_i)_{jk} - \langle \hat{J}_i \rangle_\psi \right)^2 dt + \sum_{i=1}^3 \left((\hat{J}_i)_{jk} - \langle \hat{J}_i \rangle_\psi \right) d\xi_i \right\} c_k, \end{aligned} \quad (22)$$

where $(\hat{X})_{jk} \equiv \langle \psi_j(0) | \hat{X} | \psi_k(0) \rangle$ and

$$C_{jk} \equiv \langle \psi_j(0) | \psi_k(0) \rangle \quad (23)$$

is the overlap matrix. It should be noted that the overlap matrix is time-independent.

The unitary transformation \hat{T}_2 is not unique and serves to rotate the state in such a manner that the rotated state is localized in the fixed basis. In the simulation we use an initial spin-coherent state $|-j\rangle$, represented by the point at the south pole of the phase-space. Accordingly, the fixed basis of M states is localized about the south pole. Therefore, the unitary transformation \hat{T}_2 has to ensure that the expectation values of \hat{J}_x and \hat{J}_y in the rotated state vanish. As pointed out in Section II C, in the Hilbert-Schmidt picture this rotation corresponds to rotation of the density operator in such a way that its projection on the SGA of the single-particles observables is proportional to \hat{J}_z . \hat{T}_2 is not unique. In our simulations \hat{T}_2 is chosen to be a unitary transformation, generated by \hat{J}_x and \hat{J}_y . Since \hat{T}_2 is generated by the $\mathfrak{su}(2)$ SGA itself, the transformation (19) of the single-particle observables and the Hamiltonian is performed analytically at each time-step.

2. The choice of numerical values

A converged solution is independent of the numerical parameters in the Eq.(22). They include the parameters of the basis, its size M , the strength of the measurement γ and the

size of the time-step dt . The convergence is obtained by increasing M and dt and decreasing γ .

3. Choice of basis

The choice of the basis is practically determined by its size M . In fact, a solution of the sNLSE is localized in the phase-space under the action of the noise [13, 14]. Therefore, a localized basis of states is sufficient to represent the solution. A set of $N + 1$ spin-coherent states comprises the full basis of the Hilbert space. A spin-coherent state is represented by a point on the (phase-space) sphere. A natural choice is a uniform distribution of the points on the sphere. A state, localized in an area A on the sphere can be represented by $M = (N + 1)A/4\pi$ points uniformly distributed on the area A . In practice, a more dense sampling has proved to be advantageous for the numerical stability of the solution.

The value of M in the convergent solution depends on the strength of the measurement γ . It can be estimated for $U/\omega = O(1)$:

$$M \lesssim \frac{2\omega}{\gamma N} \quad (24)$$

provided $M \gg 1$. As γ goes to zero M approaches its value in the corresponding unitary dynamics which in the strong interaction regime may become of the order of N . The convergent (in γ) solution is obtained when $\gamma \ll \omega/N$ [see subsection (III B 5) below]. The value of M in (24) is determined by $\gamma_\epsilon \equiv \epsilon\omega/N$, $\epsilon \ll 1$:

$$M \lesssim \frac{2\omega}{\gamma_\epsilon N} = O(\epsilon^{-1}), \quad (25)$$

i.e., for convergency it is sufficient that $M \gg 1$. It follows that the solution of the sNLSE can be represented efficiently at γ_ϵ .

4. Choice of a time-step

From the Eq.(22) the size of the time-step should be chosen to ensure that the spectral norm of the Hamiltonian satisfies $|\hat{H}| \ll dt^{-1}$. An estimate for the spectral norm is given by the inverse of the characteristic time scale of the dynamics, which for $U/\omega = O(1)$ is of the order of ω . As N goes to infinity the area in the phase space, corresponding to the localized

basis for any fixed M decreases as $1/N$, i.e., its linear dimension decreases as $1/\sqrt{N}$. On the time interval dt the localized state is expected to move the distance of $dt\omega$ on the sphere. For the infinitesimal transformation the state must remain localized in the basis. Therefore, it is necessary that

$$\omega dt \ll O(1/\sqrt{N}). \quad (26)$$

It follows that the simulation on the time interval of ω^{-1} must take no less than $O(\sqrt{N})$ time-steps.

The expectation of the term $\gamma \sum_{i=1}^3 \left(\hat{J}_i - \langle \hat{J}_i \rangle_\psi \right)^2$ in Eq.(22) in a localized state is of the order of $O(\gamma NM)$ [13]. Since $O(\gamma NM) = O(\omega)$, as follows from Eq.(24), this term is sufficiently small at $dt = O(1/\sqrt{N})$.

The operator in the stochastic term of Eq.(22), $\sum_{i=1}^3 \left(\hat{J}_i - \langle \hat{J}_i \rangle_\psi \right)$, has spectral norm of the order of N . Therefore, we must have $d\xi_i N \ll 1$. Using Eqs.(15) and (24) we obtain $dt\gamma \ll O(1/N^2)$ and, finally

$$\omega dt \ll O(1/N), \quad (27)$$

which leads to the number of time-steps on the time interval of ω^{-1} of the order of $O(N)$. It follows that the linear implementation of the algorithm is not efficient in the sense of the definition in Section II.

5. Choice of γ

In order that the effect of noise on the dynamics of \hat{J}_i can be neglected on the time-scale of $O(\omega^{-1})$ it is necessary and sufficient that the growth of the total uncertainty (in the observed dynamics) due to the noise is negligible on the time-scale of $O(\omega^{-1})$, as compared to the uncertainty of the initial spin-coherent state, i.e., the minimal uncertainty [26]:

$$\gamma \ll \frac{\omega}{N} \quad (28)$$

Therefore, the open-system dynamics of the single-particle observables converges to the original unitary evolution at the strength of noise $\gamma_\epsilon = \epsilon \frac{\omega}{N}$, $\epsilon \ll 1$.

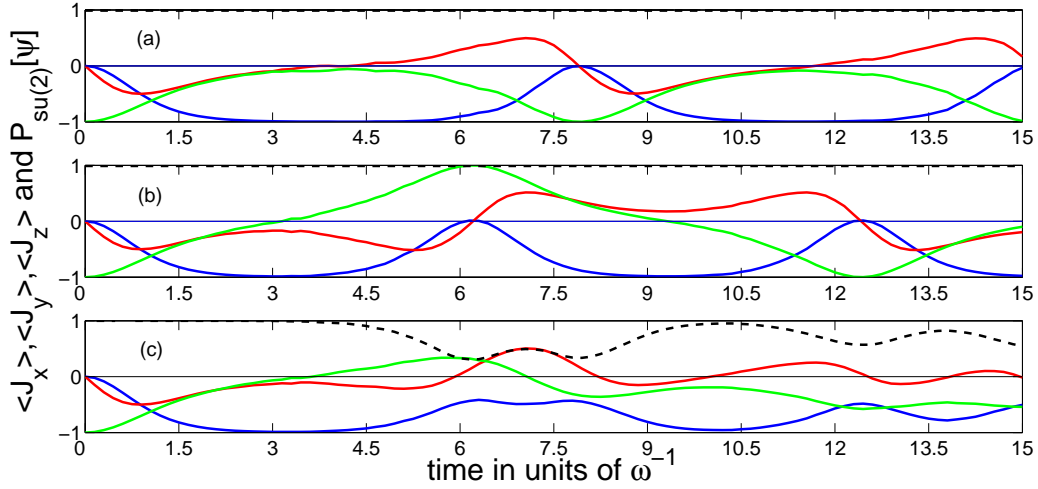


FIG. 3: (Color online). Panels (a) and (b) display the (normalized by the factor $j = N/2$) expectation values of the single-particle observables \hat{J}_x (blue, solid), \hat{J}_y (red, solid) and \hat{J}_z (green, solid), Eq.(2), and the generalized purity (black, dashed), Eq.(16) as a function of time. The expectation values are calculated in the pure-state convergent solutions of the sNLSE (14) for two different realizations of noise. The system of $N = 2 \cdot 10^4$ atoms resides initially in a spin-coherent state corresponding to the condensate prepared in the left well of the trap. The value of the on-site interaction is chosen $U/\omega = 2$. Time is measured in units of $\omega^{-1} = 0.5\Delta^{-1}$. The size of the time-dependent basis $M = 60$. Panel (c) is the average of realizations in panel (a) and (b).

6. Numerical results

Convergence in the size of the basis can be checked on the level of a single stochastic realization of the sNLSE (14). Figure 3) (a) and (b) displays dynamics of the single-particle observables for two different realizations of noise in Eq.(14). The size of the basis is $M = 60$ and the value of γ is $0.5/N$. The strong localization results in the values of the generalized purity indistinguishable from unity as in a single spin-coherent state. The two trajectories coincide on a short time interval, corresponding to high generalized purity of the exact solution (Fig(4)). On this short time interval the mean-field solution (Cf.Fig(2)) is a perfect approximation. Starting at $t \approx 2\omega^{-1}$ the two trajectories start to diverge abruptly. Each simulation takes a couple of minutes on a PC.

Figure 3) (c) shows the dynamics of the single-particle observables averaged over the two realizations and the corresponding generalized purity . The main feature is an apparent

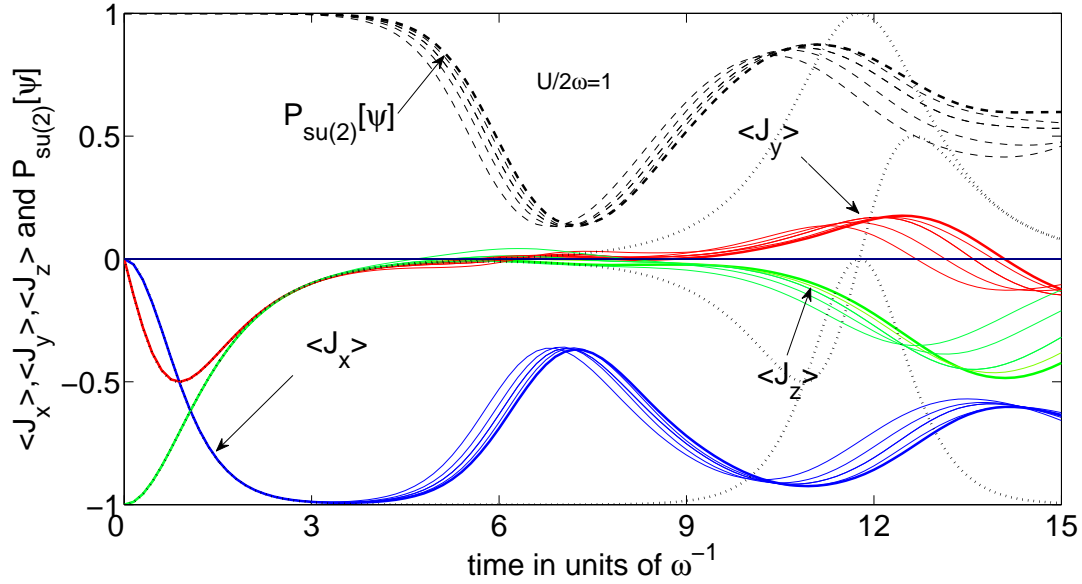


FIG. 4: (Color online). The (normalized by the factor $j = N/2$) expectation values of the single-particle observables \hat{J}_x (blue, solid), \hat{J}_y (red, solid) and \hat{J}_z (green, solid), Eq.(2), and the generalized purity (black, dashed), Eq.(16) as a function of time. The system of $N = 2 \cdot 10^4$ atoms resides initially in a spin-coherent state corresponding to the condensate prepared in the left well of the trap. The value of the on-site interaction in the Hamiltonian (3) is chosen $U/\omega = 2$. Time is measured in units of ω^{-1} . The plots for five values of the measurement strength are presented: $\gamma = 8/N, 4/N, 2/N, 1/N$ (thin lines), $0.5/N$ (thick line). The expectation values are averages of 2000 stochastic pure-state convergent solutions of the sNLSE (14) for each value of γ . The size of the time-dependent basis $M = 60$ in the convergent solution. The mean-field solution (black, dotted) is presented for comparison.

decrease of the generalized purity. This implies that some features of a many-body dynamics are attainable from a small number of realizations.

Averaging over 2000 stochastic trajectories leads to a relative error of 2.5% for the expectation values of the observables. Figure (4) presents the averaged results. The averaging has been performed for solutions of the sNLSE, corresponding to $\gamma = 8/N, 4/N, 2/N, 1/N$ and, finally, to $\gamma = 0.5/N$ at which the convergence to the unitary evolution becomes apparent. The evolution on the time interval $0 < t < 2\omega^{-1}$ corresponds to the mean-field behaviour and is not visibly perturbed by the measurement. The size of the basis for the convergent solution is $M_{sNLSE} = 60$.

The size of the basis necessary to span the pure-state evolution, governed by the original Schrödinger equation can be estimated from Figure (4). The minimal purity obtains at $t \approx 7.5\omega^{-1}$. Its (normalized) value at this point is $P_{\mathfrak{su}(2)}[\psi] \approx 0.13$ which corresponds to

$$M_{SE} = (N + 1) \left(1 - \sqrt{P_{\mathfrak{su}(2)}[\psi]} \right) \approx 0.64N, \quad (29)$$

where the formula derived in Ref.[13] is used.

Therefore, the size of the time-dependent basis is compressed by the factor of $M_{SE}/M_{sNLSE} \approx 2 \cdot 10^2$! As a result, the memory cost is reduced by the factor of $4 \cdot 10^4$. The number of the time-steps for the propagation is $2 \cdot 10^6$, which results in reduction of the CPU resources by the factor of 10^3 .

IV. CONCLUSIONS AND DISCUSSION

An algorithm for simulation of a many-body dynamics, generated by a $\mathfrak{su}(2)$ -Hamiltonian has been described, analyzed and applied to simulation of the dynamics of cold atoms in the double-well trap. The dynamics reflects a competition between the hopping rate of the atoms from well to well and the two-body repulsive interaction between the particles. The single-particle observables of the system were simulated in the strong interaction regime and the convergence of the simulation was checked.

The simulation is based on numerical solution of the stochastic Nonlinear Schrödinger Equation (sNLSE), corresponding to weak measurement of the elements of the spectrum-generating $\mathfrak{su}(2)$ algebra (SGA) of the single-particle observables. Dynamics of the smooth SGA observables is negligibly affected by sufficiently weak measurement, which is nonetheless strong enough to localize solutions of the sNLSE in the corresponding phase-space.

The localization leads to substantial reduction of the computational complexity of the many-body dynamics. The algorithm is applied to simulation of the single-particle observables of a system of $N = 2 * 10^4$ cold atoms in a double-well trap. The localization allows to describe the pure-state solution of sNLSE by a superposition of only 60 spin-coherent states, which is smaller by the factor of $2 \cdot 10^2$ than the size of the spin-coherent basis necessary to span the solution of the original Schrödinger equation on the corresponding time interval. This "compression" of the time-dependent basis results in dramatic reduction of the computational complexity of the simulation.

The following important question is left for future investigations: can a *nonlinear implementation* of the method provide an efficient simulation of the SGA observables in the sense of definition in Section II A 1? This question is raised by the estimation performed in Section III B 6, according to which the number of time-steps of the simulation scales linearly with the number of particles (the Hilbert space dimension) N on a fixed time interval. This implies that the linear implementation of the algorithm is not efficient in the sense of our definition, according to which the computational resources of an efficient simulation do not depend on the Hilbert space representation of the SGA. The estimation has been performed in the special case of the $\mathfrak{su}(2)$ SGA but can be generalized to an arbitrary compact semisimple algebra of observables with a similar result. It is possible that the scaling with N is a drawback of the linear implementation of the method. An algorithm based of solving nonlinear equations of motion, corresponding to the situation where each element of the time-dependent basis follows its own unitary evolution, may have a different scaling.

Acknowledgments

We thank Uri Heinemann and Shimshon Kallush for help in programming. Work supported by DIP and the Israel Science Foundation (ISF). The Fritz Haber Center is supported by the Minerva Gesellschaft für die Forschung GmbH München, Germany.

-
- [1] W. Kohn, *Nobel Lecture* (January 28, 1999).
 - [2] A. J. Leggett, *Rev. Mod. Phys.* **73**, 307 (2001).
 - [3] T. Schumm, S. Hofferberth, L. Andersson, S. Wildermuth, S. Groth, I. Bar-Joseph, J. Schmiedmayer, and P. Kruger, *Nature Physics*. **1**, 57 (2005).
 - [4] R. Gati, B. Hemmerling, J. Fölling, M. Albiez, and M. K. Oberthaler, *Phys. Rev. Lett.* **96**, 130404 (2006).
 - [5] R. Gati and M. K. Oberthaler, *J. Phys B: At. Mol. Phys.* **40**, R61 (2007).
 - [6] G. D. Mahan, *Many-particle physics* (Kluwer Academic/Plenum Publishers, New York, 2000).
 - [7] A. Bohm, Y. Neeman, and A. O. Barut, *Dynamical groups and spectrum generating algebras* (World Scientific, Singapur, 1988).

- [8] W. Zhang, D. H. Feng, and R. Gilmore, *Rev. Mod. Phys.* **62**, 867 (1990).
- [9] R. Kosloff, *J. Phys. Chem.* **92**, 2087 (1988).
- [10] N. Gisin, *Phys. Rev. Lett.* **52**, 1657 (1984).
- [11] L. Diosi, *Physics Letters A* **129**, 419 (1988).
- [12] N. Gisin and I. C. Percival, *J. Phys A: Math.Gen.* **25**, 5677 (1992).
- [13] M. Khasin and R. Kosloff, *Phys. Rev. A* **78**, 012321 (2008).
- [14] M. Khasin and R. Kosloff, *J. Phys A: Math.Gen.* **41**, 365203 (2008).
- [15] P. Kramer and M. Saraceno, *Geometry of the Time-Dependent Variational Principle in Quantum Mechanics* (Springer-Verlag, Berlin, 1981).
- [16] A. Perelomov, *Generalized Coherent States and their Applications* (Springer, Berlin, 1985).
- [17] A. Peres, *Quantum Theory: Concepts and Methods* (Kluwer, Boston, 1998).
- [18] H. Barnum, E. Knill, G. Ortiz, and L. Viola, *Phys. Rev. A* **68**, 032308 (2003).
- [19] H. J. Lipkin, N. Meshkov, and A. Glick, *Nucl. Phys.* **62**, 188 (1965).
- [20] A. Vardi and J. R. Anglin, *Phys. Rev. Lett.* **86**, 568 (2001).
- [21] F. Trimborn, D. Witthaut, and H. J. Korsch, *Phys. Rev. A* **77**, 043631 (2008).
- [22] F. Arecchi, E. Courtens, R. Gilmore, and H. Thomas, *Phys. Rev. A* **6**, 2211 (1972).
- [23] I. Tikhonenkov, J. R. Anglin, and A. Vardi, *Phys. Rev. A* **75**, 013613 (2007).
- [24] V. Viera and P. Sacramento, *Ann. Phys.* **242**, 188 (1995).
- [25] Y. Khodorkovsky, G. Kurizki, and A. Vardi, *Phys. Rev. Lett.* **100**, 220403 (2008).
- [26] M. Khasin and R. Kosloff, in preparation.
- [27] H. Tal-Ezer and R. Kosloff, *J. Chem. Phys.* **81**, 3967 (1984).